Proceedings of the Canadian Society for Mechanical Engineering International Congress
Computational Fluid Dynamics Canada International Congress
CSME - CFD-SC2023
May 28-31, 2023, Sherbrooke, QC, Canada

1D MODELLING OF THE LIQUID-GAS JET PUMP PERFORMANCE

Akbar Ravan Ghalati[1*], Sergio Croquer[2], Hakim Nesreddine[3], Sébastien Poncet[2], Jay Lacey[1]
[1]Civil & Building Engineering Department, Université de Sherbrooke, Sherbrooke, Canada
[2]Mechanical Engineering Department, Université de Sherbrooke, Sherbrooke, Canada
[3]Laboratoire des technologies de l'énergie, Hydro-Québec, Shawinigan, Canada
*akbar.ravan.ghalati@usherbrooke.ca

Abstract—The performance of a liquid-gas jet pump, which uses a high-velocity liquid flow to compress and entrain a gas flow, can be divided into two modes; on-design and off-design. The present paper investigates the mentioned modes of performance using a 1D model based on the conservation equations of mass, momentum and energy. Comparisons in terms of compression ratio and efficiency between the present model and experimental data show that the 1D model is capable of predicting the behavior of the liquid-gas jet pump for both modes. The effects of the primary flow velocity head, and areas of the mixing throat and diffuser on the performance of the jet pump are also investigated through a sensitivity study.

Keywords: jet pump; 1D numerical model; liquid-gas flow; compression ratio; efficiency

I. INTRODUCTION

Jet pumps are devices without any moving parts, that transfer energy from a primary (motive) fluid to a secondary (driven) fluid [1]. As it is schematically shown in Fig. 1, the jet pump consists of four main components, namely: nozzle, suction chamber, mixing throat and diffuser. The high-pressure primary fluid with certain energy is discharged into the mixing throat by the nozzle at a high speed, and the air is taken away to form a vacuum negative pressure state near the nozzle. The low-pressure forces the secondary fluid into the pump through the suction pipe, and then the secondary fluid enters the mixing chamber together with the high-speed primary fluid. In the mixing throat, the primary fluid with high-pressure will transfer part of its kinetic energy to the secondary fluid with low-pressure while the two flows are mixing together. Then the mixed fluid is introduced into the diffuser where its pressure is gradually increased [2]. The condition in which the primary and secondary fluid will not mix in the mixing throat is termed as off-design mode, as will be explained later in this paper.

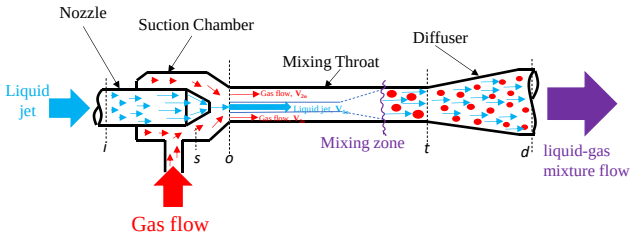

Figure 1. Schematic representation of flow in a liquid-gas jet pump operating in on-design mode.

Jet pumps have been widely utilized because of their simplicity and high reliability, absence of lubricants or bearings [3] and low installation costs [4] in broad areas including thermal energy refrigeration systems [5] and city central heating systems [6]. Jet pumps can be employed for transportation of liquids which contain solid particles or fish [7] and also hazardous liquids [8].

1D analysis of the jet pump performance using the conservation of mass, momentum and energy equations is an efficient method in terms of computational costs. Additionally, the reliability of this method has been confirmed by previous studies. Winoto et al. [9] performed a combined theoretical and experimental analysis of the jet pump efficiency of jet pumps, using liquid water for both the primary and secondary streams. It was concluded that using non-circular nozzles for liquid-liquid jet pumps increases energy losses and lowers the efficiency of the pump. They also concluded that the performance of the water jet pump can be adequately described using 1D theoretical formulation. De Oliveira Marum et al. [10] performed axisymmetric CFD simulations to calculate the friction loss coefficients of each part of the water jet pump by fitting the CFD data to a quasi-1D mathematical model adapted from [9]. The efficiency, static pressure profile along the length of the jet pump and static pressure at different radial cross sections were calculated by CFD model coupled with various turbulence models. By comparing the numerical data obtained using k-ε, k-ω and k-ω SST turbulence models with experimental results, it was concluded that k-ω SST model is the most suitable to capture the ejector's flow characteristics in all operational

conditions, especially the peak-efficiency operational condition. De Oliveira Marum et al. [10] mentioned that the accuracy of the k-ω model was unsatisfactory. A high-pressure water jet was used by Cunningham [11] as the primary flow to compress air. The 1D model was validated by experimental data. The author concluded that the efficiency of liquid-air jet pumps can be as high as for liquid-liquid jet pumps if a mixing throat with enough length is used. Cunningham [11] concluded that if mixing of water and air does not occur in the mixing throat, the jet pump efficiency would decrease drastically. Cunningham and Dopkin [12] experimentally investigated the effects of the design parameters (including mixing throat length, nozzle-throat area ratio, nozzle contour, spacing, jet velocity and suction pressure) on the mixing location inside the mixing throat for a water-air jet pump. Through a parametric analysis, they deduced an empirical formula based on the design parameters for the required length of the mixing throat (which ensures the full mixing of the two flows in the mixing throat). Witte [13] investigated the mixing phenomenon in the mixing throat and concluded that employing a multi-hole nozzle in a liquid-gas jet pump increases its efficiency. In another study, Witte [14] showed that the efficiency of the liquid-gas jet pump (within the range of the experimented data) can reach up to 45% as long as the mixing location is situated in the mixing throat. The experimental set-up in Witte [14] included a Knock-out Drum: a device located after the diffuser to separate the liquid and gas phases and send the liquid phase to the nozzle inlet through a pump. It was concluded that by integrating a Knock-out Drum to the system, the jet pump operates in a closed circuit and its efficiency is higher than operating in an open system. Zhang et al. [15] recently reviewed the research and application status of liquid gas jet pumps, and highlighted the superiority and irreplaceability of these devices in many technological processes.

The previous literature review demonstrates that 1D modelling of jet pumps is a feasible design approach for these devices. The previous studies employed 1D modelling to predict the liquid-gas performance only when the mixing of the two flows occurs within the mixing throat or, in other words, when the jet pump operates in the on-design mode. However, operating in the off-design mode can occur if the operating conditions are different from the design conditions. The off-design mode efficiency is considerably lower than the on-design mode. This drawback is attributed to the static configuration of the device which leads to show the best performance in a single operating point, while being less efficient away from that point [16].

The present study aims to reflect the on-design and off-design behaviors of liquid-gas jet pumps using conservation equations. A sensitivity analysis is also carried out to investigate the effects of various design parameters, including the primary flow velocity head, the area of the mixing throat and the area of the diffuser on the jet pump performance.

II. Theoretical Analysis

The following assumptions are considered in the developed 1D mathematical model:

- Water is the primary fluid and gas is the secondary fluid.
- Gas is compressed isothermally from section *s* to section *d* (cross sections are shown Fig. 1).
- There is no pressure or temperature change in the gas flow at the jet pump entry (i.e., from section *s* to *o*).
- Any change in water temperature is neglected.
- Once the gas and water flows are mixed, a homogeneous bubbly mixture flow is created in which there is no slip between the two phases.
- The distance between the nozzle outlet and the mixing section inlet is zero.
- The pressure is uniform at any cross section along the jet pump.
- Gas flow is assumed to behave as an ideal gas.

Application of conservation equations considering the mentioned assumptions in each component of the jet pump leads to an expression for the calculation of the liquid-gas jet pump efficiency.

A. On-design mode

When the liquid and gas phases mix in the mixing throat, the jet pump is operating in the on-design mode. The governing equations for the flow inside the device are shown below.

1) Nozzle

Energy equation for the nozzle can be expressed as:

$$P_{1i} + \frac{\rho_1 V_{1i}^2}{2} = P_{1o} + \frac{\rho_1 V_{1o}^2}{2} + \frac{K_{nz}\rho_1 V_{1o}^2}{2} \quad (1)$$

where P_i and P_o are the static pressures at the nozzle inlet and outlet, respectively. V_{1i} is the velocity of the primary flow at the nozzle inlet, V_{1o} is the velocity of the primary flow at the cross-section *o* and K_{nz} is the friction loss coefficient of the nozzle. ρ_1 is the density of the primary fluid.

By replacing the total pressure of the primary fluid at the nozzle inlet $\overline{P_{1i}}=P_{1i}+\rho_1 V_{1i}^2/2$ in Eq. (1), the nozzle equation becomes:

$$\overline{P_{1i}} - P_{1o} = Z\,(1+K_{nz}) \quad (2)$$

where $Z=\rho_1 V_{1o}^2/2$ is the jet velocity head.

2) Suction chamber

The assumption of negligible pressure drop in the suction chamber for the gas flow leads to:

$$P_{1s}=P_{1o} \quad (3)$$

Additionally, due to the assumption of pressure uniformity in all cross-sections, the pressure at the mixing chamber inlet is denoted by P_o in the following.

3) Mixing throat

The momentum equation for the mixing throat (from sections *o* to *t*) can be express as:

$$(P_o - P_t)A_t - \tau A_w = (\dot{m}_1 + \dot{m}_2)V_{3t} - [\dot{m}_1 V_{1o} + \dot{m}_2 V_{2o}] \quad (4)$$

where $\dot{m}_1$ and $\dot{m}_2$ are the mass flow rates of the primary and secondary flows, V_{3t} is the velocity of the mixed flow at the mixing throat outlet, P_t is the static pressure at the mixing section outlet, τ is the shear stress, A_t and A_W are the cross-sectional area and internal wall area of the mixing throat, respectively.

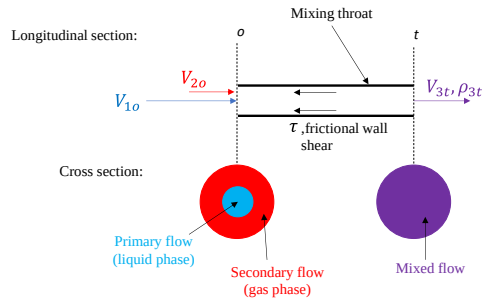

Figure 2. Longitudinal and cross sections of the mixing throat.

Considering $\dot{m}=\rho AV$, Eq. (4) can be written as:

$$(P_o - P_t)A_t - \tau A_w = \rho_{3t} V_{3t}^2 A_t - \rho_1 V_{1o}^2 A_n - \rho_{2o} V_{2o}^2 A_{2o} \quad (5)$$

where A_n and A_{2o} are the nozzle area and the area occupied by the secondary flow at *o* section, respectively. The density and velocity of the mixture flow at the end of the mixing throat are calculated by:

$$\rho_{3t} = \frac{\dot{m}_1+\dot{m}_2}{Q_1+Q_2} = \rho_1 \frac{\left(1+{}^{\dot{m}_1}/_{\dot{m}_2}\right)}{1+\varphi_t} = \rho_1 \frac{1+\gamma\varphi_o}{1+\varphi_t} \quad (6)$$

$$V_{3t} = \frac{Q_{3t}}{A_t} = \frac{Q_1+Q_2}{A_t} = \frac{Q_1(1+\varphi_t)}{A_n * {}^1/_b} = V_{1o} b(1+\varphi_t) \quad (7)$$

where $\varphi = Q_2/Q_1$ is the volumetric flow ratio (at various sections: o, t, d), $\gamma = \rho_{2o}/\rho_1$ is the density ratio and $b = A_n/A_t$ is the nozzle to mixing throat area ratio. With $\varphi_t = P_o\varphi_o/P_t$ and $\tau 4L/D_t = k_{th}\,\rho_{3t}V_{3t}^2/2$, the pressure rise in the mixing chamber (Eq. (5)) can be written as:

$$P_t^2 - \left[Z\left(2b - b^2(2+k_{th})(1+\gamma\varphi_o) + 2\gamma\varphi_o^2 \tfrac{b2}{1-b}\right) + P_o\right]P_t + Z[(2+k_{th})b^2(1+\gamma\varphi_o)\,\varphi_o P_o] = 0 \quad (8)$$

4) Diffuser

A homogeneous mixture enters the diffuser at P_t and V_{3t}, and decelerates to V_{3d} and pump discharge pressure P_d. The Euler equation of motion for the mixture flow in the diffuser writes:

$$\frac{dP}{\rho_3} + VdV + d\left[K_{dif}\frac{V_{3t}^2}{2}\right] = 0 \quad (9)$$

where K_{dif} is the friction loss coefficient of the diffuser. Using the ideal equation of state, the density of the mixture through the diffuser can be expressed as a function of pressure as:

$$\rho_3 = \rho_1 \left(\frac{1+\gamma\varphi_o}{1+\frac{P_o\varphi_o}{P}}\right) \quad (10)$$

The integration of the motion equation along the diffuser (from cross-sections *t* to *d*) yields:

$$P_d - P_t = Z(1+\gamma\varphi_o)[b^2 + (1+\varphi_t)^2 + a^2b^2(1+\varphi_d)^2 - K_{di}b^2(1+\varphi_t)] - P_o\varphi_o \mathrm{Ln}\left({}^{P_d}/_{P_t}\right) \quad (11)$$

5) Jet pump efficiency

The efficiency of the liquid-gas jet pump is defined as:

$$\eta_{jp} = W_{out}/e_{in} \quad (12)$$

where W_{out} is the useful work output rate (isothermal compression of an ideal gas from P_s to P_d), and e_{in} is the input energy rate. These terms are defined by:

$$W_{out} = Q_{2s}\frac{P_s}{\rho_s}\ln\left(\frac{P_d}{P_s}\right) \quad (13)$$

$$e_{in} = Q_1(\bar{P}_i - P_d) \quad (14)$$

B. Off-design mode

When the liquid jet leaves the mixing throat without mixing with the gas flow, the liquid-gas jet pump operates in the off-design mode. The governing equations of the flow inside the device are written below. It must be noted that equations for the nozzle, suction chamber and jet pump efficiency are similar to the equations mentioned in the previous section and are not repeated here for brevity.

1) Mixing throat

Conservation of mass, energy and momentum for the water jet in the mixing throat can be expressed by Eqs (15), (16) and (17), respectively:

$$V_{1o}A_n = V_{1t}A_{1t} \quad (15)$$

$$P_o + \frac{\rho_1 V_{1o}^2}{2} = P_t + (1+k_{th})\left(\frac{\rho_1 V_{1t}^2}{2}\right) \quad (16)$$

$$(P_oA_{1o} - P_tA_{1t}) - k_{th}\left(\frac{\rho_1 V_{1t}^2}{2}\right)A_{1t} = (\rho_{1o}V_{1o}A_n)[V_{1t} - V_{1o}] \quad (17)$$

2) Diffuser

Fig. 3 schematically shows the fluid flow and exerted forces in the diffuser when the liquid-gas jet pump operates in the off-design mode.

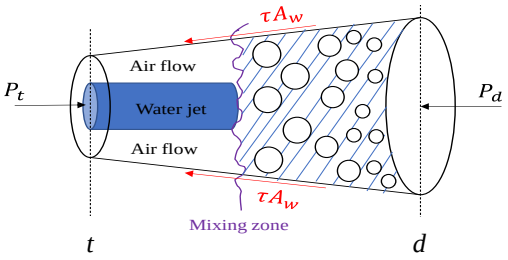

Figure 3. Schematic representation of the fluid flow behaviour in the diffuser in the off-design mode.

The conservation of momentum in the diffuser can be expressed by:

$$(P_t A_t - P_d A_d) - \tau A_w = (\dot{m}_1 + \dot{m}_2) V_{3d} - [\dot{m}_1 V_{1t} + \dot{m}_2 V_{2t}] \quad (18)$$

Considering $\dot{m}=\rho A V$ and $\tau A_w = k_{th}\, \rho_{3d} \frac{V_{3d}^2}{2} A_d$, Eq. (18) can be written as:

$$(P_t A_t - P_d A_d) - k_{dif} \frac{\rho_{3d} V_{3d}^2}{2} A_d = (\rho_{3d} V_{3d}^2 A_d) - (\rho_1 V_{1t}^2 A_{1t}) - (\rho_{2t} V_{2t}^2 A_{2t}) \quad (19)$$

where ρ_{3d} and V_{3d} are the density and velocity of the liquid-gas mixture at the outlet of the diffuser and can be defined by Eqs (20) and (21), respectively.

$$\rho_{3d} = \rho_1 \frac{1+\gamma\varphi_o}{1+\gamma\varphi_d} \quad (20)$$

$$V_{3d} = \frac{Q_1(1+\varphi_d)}{\frac{A_n}{ab}} \quad (21)$$

where $a = A_t/A_d$ and $\varphi_d = \frac{P_o \varphi_o}{P_d}$.

III. VALIDATION

Experimental results for a liquid-air jet pump reported by Cunningham and Dopkin [12] are used to validate the 1D mathematical model. Fig. 4 shows the pressure ratio in the mixing throat $R_{to} = P_t/P_o$ and diffuser $R_{ds} = P_d/P_s$ as a function of the flow ratio φ_o, which is an independent variable. In Ref. [12] various flow ratios were achieved by adjusting the discharge pressure P_d.

The entrained air flow in the jet pump is compressed in two stages; i.e., in the mixing throat and diffuser as shown in Fig. 4a and Fig. 4b. The jet pump operates in the on-design mode up to the point when there is a sharp change in the slope of R_{to} and R_{ds}. Further reducing the value of P_d beyond this point leads to less air compression and more entrained air flow.

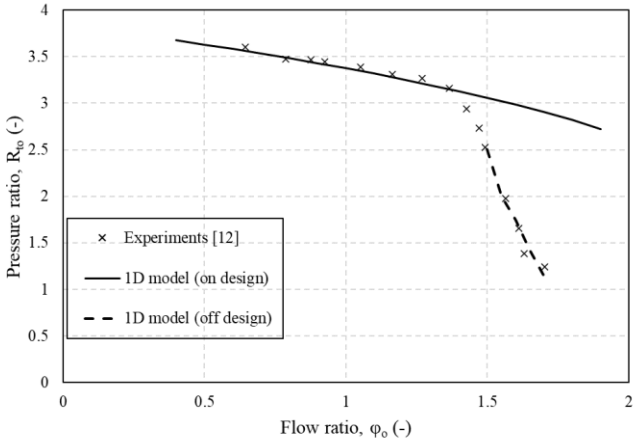

(a)

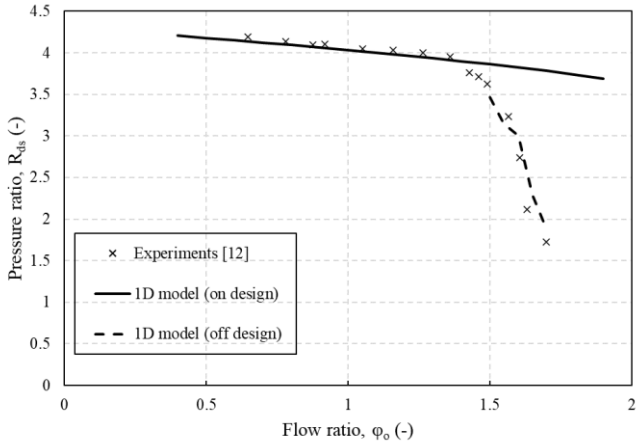

(b)

Figure 4. Pressure ratio against the flow ratio for (a) the mixing throat and (b) the jet pump. Comparisons between the predictions of the 1D model and the experimental data of Cunningham and Dopkin [12] for both on- and off-design regimes.

Fig. 5 displays the efficiency of the jet pump as a function of the flow ratio. As seen in Eq. (12), the efficiency of the jet pump is the product of the flow ratio by the pressure ratio. As long as the mixing zone is located in the mixing chamber, increasing the flow ratio leads to higher efficiency. Once the mixing zone moves into the diffuser, i.e. the jet pump operates in the off-design mode, the efficiency decreases sharply with increasing the volume of air entrained in the jet pump.

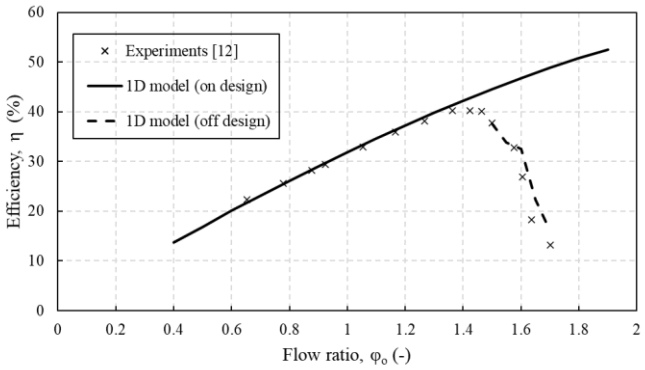

Figure 5. Jet pump efficiency against the flow ratio. Comparisons between the predictions of the 1D model and the experimental data of Cunningham and Dopkin [12] for both on- and off-design regimes.

By looking at Figs 4 and 5, it can be concluded that the 1D numerical model is in fairly good agreement with the experimental data of Cunningham and Dopkin [12] for both on- and off-design modes. The maximum discrepancy between the experimental and numerical values of the pressure ratio in the mixing throat and the diffuser are 7% and 9%, respectively. The maximum difference in terms of jet pump efficiency is 23%. The stated errors are related to the off-design mode. The discrepancy of all parameters in the on-design mode is less than 5% in comparison to the experimental data.

IV. Results and Discussion

This section focuses on the influence of some design parameters, including the jet velocity head, mixing throat diameter and exit diameter of the diffuser on the performance of a water-air jet pump. In the following sensitivity analysis, every parameter is kept constant except the parameter of interest.

The efficiency curve and the pressure ratio of the water-air jet pump operating with three values of the jet velocity head i.e., Z= 345, 666 and 1034 kPa, are displayed in Figs 6 and 7, respectively. It shows that discharging a primary jet with higher velocity head causes more compression and less efficiency. Higher compression ratio is due to the ability of the jet with higher velocity head to transfer more momentum to the secondary phase. Increasing the velocity head of the primary fluid can be interpreted as increasing the numerator and denominator of Eq. (12) at the same time. Since the increase in e_{in} is higher than in W_{out} while increasing Z, the jet pump with more velocity head is less efficient (Fig. 6). Consequently, if more compression ratio is needed, it can be achieved at the expense of operating with less efficiency.

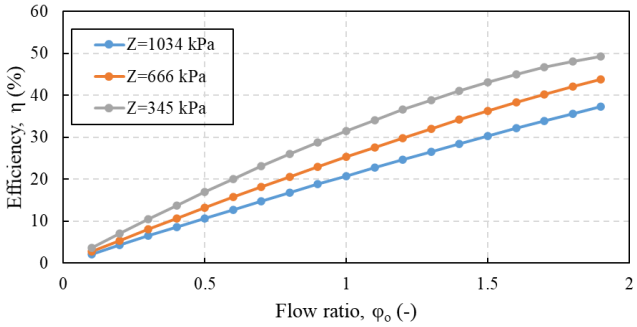

Figure 6. Jet pump efficiency as a function of the flow ratio for three values of the primary flow velocity head. Results obtained by the 1D model.

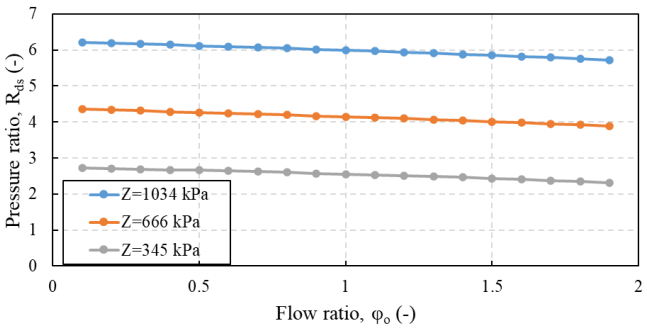

Figure 7. Pressure ratio of the jet pump as a function of the flow ratio for three values of the primary flow velocity head. Results obtained by the 1D model.

The efficiency curve and the pressure ratio of the water-air jet pump operating with three values of the nozzle-to-throat area ratio i.e., b=A_n/A_t = 0.3, 0.2 and 0.1, are shown in Figs 8 and 9, respectively. It must be noted that decreasing the value of the parameter b when the value of the velocity head, *Z*, is constant can be interpreted as increasing the area of the mixing throat, A_t.

As shown in Fig. 8, increasing the diameter of the mixing throat causes efficiency drop with the same flow ratio or back pressure, P_d. The reason behind this phenomenon can be seen in Fig. 9 where increasing the diameter of the mixing throat leads to less compression ratio in the mixing throat. In other words, when there is more space around the primary flow, the gas flow will be less compressed by the momentum transfer process.

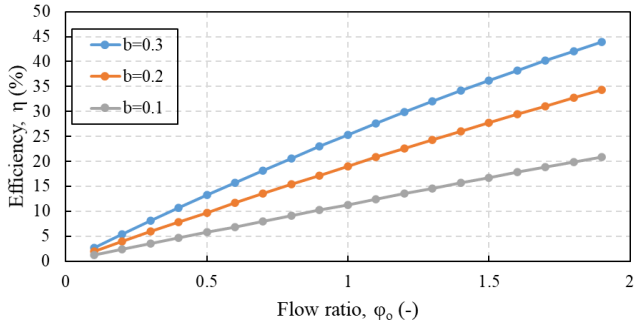

Figure 8. Efficiency of the jet pump as a function of the flow ratio for three values of the nozzle-to-throat area ratio. Results obtained by the 1D model.

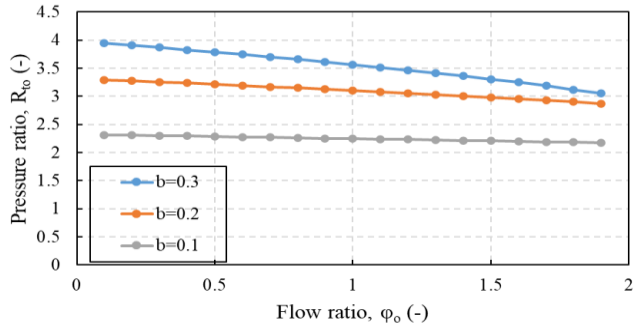

Figure 9. Pressure ratio of the mixing throat as a function of the flow ratio for three values of the nozzle-to-throat area ratio. Results obtained by the 1D model.

The efficiency curve and the jet pump pressure ratio of the liquid-air jet pump operating with three values of the throat-to-diffuser area ratio i.e., a=A_t/A_d=0.7, 0.235 and 0.05, are shown in Figs 10 and 11, respectively. It must be noted that changing the value of the parameter *a* when the area of the mixing throat is constant can be interpreted as changing the outlet area of the diffuser, A_d.

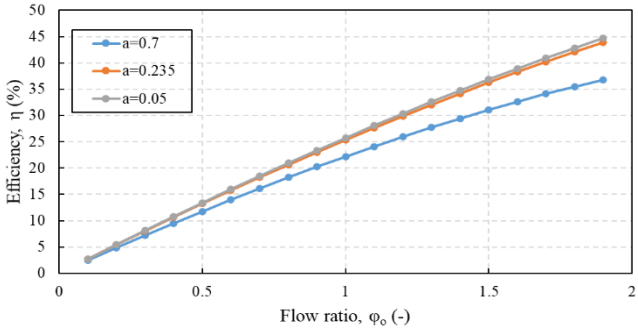

Figure 10. Efficiency of the jet pump as a function of the flow ratio for three values of the throat-to-diffuser area ratio. Results obtained by the 1D model.

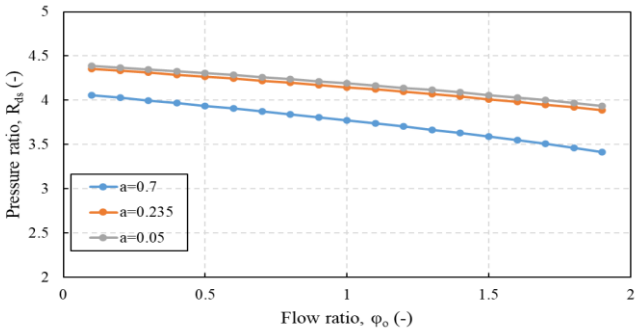

Figure 11. Pressure ratio of the jet pump as a function of the flow ratio for three values of the throat-to-diffuser area ratio. Results obtained by the 1D model.

As shown in Fig. 10, changing a=0.235 (the value used in [11]) to a=0.05 leads to marginal efficiency gain. However, decreasing the outlet area of the diffuser to a=0.7 causes considerable efficiency loss for the same air flow entrained by the jet pump. The underlying reason for this behavior could be the modification of the compression ratio due to a change in the diffuser area as displayed in Fig. 11. It is obvious that by decreasing the outlet area of the diffuser, the air flow is less compressed in the diffuser. On the other hand, changing a=0.235 to a=0.05 does not change the compression ratio considerably. It can be due to the fact that the momentum transfer process from the primary flow to the secondary flow is almost completed when a=0.235, and increasing further the outlet area of the diffuser cannot compress the air flow noticeably. It also shows that Cunningham [11] chose the optimum value of the throat-to-diffuser for the experimental setup.

V. CONCLUSIONS

The present study investigated the performance of a liquid-gas jet pump using a 1D model for the on-design and off-design operating regimes. The following conclusions can be drawn:

- The 1D model based on the conservation equations of mass, momentum and energy can predict the performance of liquid-gas jet pumps operating in the on-design and off-design modes.
- The utilized 1D model predicts the jet pump performance in the on-design mode with less than 5% error.
- In the off-design mode, the maximum discrepancy between the experimental and numerical values of the pressure ratio in the mixing throat and the diffuser are 7% and 9%, respectively. The maximum difference in terms of jet pump efficiency in the off-design is 23%.
- Increasing the velocity head of the primary flow leads to more compression of the secondary flow and a lower efficiency of the jet pump.
- Increasing the area of the mixing throat decreases the efficiency of the jet pump since it reduces the ability of the device for compression of the gas flow around the liquid jet.
- Increasing the area of the diffuser beyond an optimum value does not improve the efficiency of the jet pump.

Experimental investigation of the internal flow field of the liquid-gas jet pump using Particle Image Velocimetry method will be conducted in future works. Additionally, the 1D theoretical model will be validated by advanced 3D CFD simulations.

ACKNOWLEDGEMENTS

The authors acknowledge the NSERC chair on industrial energy efficiency established in 2019 at Université de Sherbrooke with the support of Hydro-Québec, Natural Resources Canada and Emerson Commercial and Residential Solutions.

REFERENCES

[1] I.J. Karassik, J.P. Messina, P. Cooper and C.C. Heald, Pump handbook, McGraw-Hill Education, 2008.

[2] T. Tan, J. Liu, H. Chen and W. Lu, "Review and comparison of ejectors design methods and their application," ASME International Mechanical Engineering Congress and Exposition, paper V08AT10A087, Montreal, November 2014.

[3] A.B. Little, S. Garimella and J.P. DiPrete, "Combined effects of fluid selection and flow condensation on ejector operation in an ejector-based chiller," International Journal of Refrigeration, vol. 69, pp. 1-16, 2016.

[4] K. Shestopalov, B. Huang, V. Petrenko and O. Volovyk, "Investigation of an experimental ejector refrigeration machine operating with refrigerant R245fa at design and off-design working conditions. Part 1. Theoretical analysis," International Journal of Refrigeration, vol. 55, pp. 201-211, 2015.

[5] G. Besagni, R. Mereu and F. Inzoli, "Ejector refrigeration: A comprehensive review," Renewable and Sustainable Energy Reviews, vol. 53, pp. 373-407, 2016.

[6] Y. Peng, H. Wenju, L. Deying, L. Xiaoyu and Z. Xiping, "Application and economic analysis of water jet pump in new district heating system," Procedia Engineering, vol. 205, pp. 996-1003, 2017.

[7] L. Xiao, X. Long, L. Li, M. Xu, N. Wu and Q. Wang, "Movement characteristics of fish in a jet fish pump," Ocean Engineering, vol. 108, pp. 480-492, 2015.

[8] E. Lisowski and H. Momeni, "CFD modeling of a jet pump with circumferential nozzles for large flow rates," Archives of Foundry Engineering, vol. 10, pp. 69-72, 2010.

[9] S. Winoto, H. Li, and D. Shah, "Efficiency of jet pumps," Journal of Hydraulic Engineering, vol. 126, pp. 150-156, 2000.

[10] V.J. de Oliveira Marum, L.B. Reis, F.S. Maffei, S. Ranjbarzadeh, I. Korkischko, R. dos Santos Gioria and J. Romano Meneghini, "Performance analysis of a water ejector using Computational Fluid Dynamics (CFD) simulations and mathematical modeling," Energy, vol. 220, 119779, 2021.

[11] R. Cunningham, "Gas compression with the liquid jet pump," Journal of Fluids Engineering, vol. 96, pp. 203-215, 1974.

[12] R. Cunningham and R. Dopkin, "Jet breakup and mixing throat lengths for the liquid jet gas pump," Journal of Fluids Engineering, vol. 96, pp. 216-226, 1974.

[13] J.H. Witte, "Mixing shocks and their influence on the design of liquid-gas ejectors," PhD thesis, TUDelft, 1962.

[14] J.H. Witte, "Efficiency and design of liquid-gas ejectors," British Chemical Engineering, vol. 10, pp. 602-607, 1965.

[15] Z. Huiyan, et al., " Liquid–gas jet pump: A review," Energies, vol. 15, pp. 1-15, 2022.

[16] R. Mulley, Flow of industrial fluids: theory and equations, CRC Press, 2004.